© 2016. Published by The Company of Biologists Ltd | Development (2016) 143, 2356-2366 doi:10.1242/dev.135913

RESEARCH ARTICLE

# Adenomatous polyposis coli regulates radial axonal sorting and myelination in the PNS

**Benayahu Elbaz[1], Maria Traka[1], Rejani B. Kunjamma[1], Danuta Dukala[1], Amanda Brosius Lutz[2], E. S. Anton[3], Ben A. Barres[2], Betty Soliven[1] and Brian Popko[1,*]**

## ABSTRACT

The tumor suppressor protein adenomatous polyposis coli (APC) is multifunctional – it participates in the canonical Wnt/β-catenin signal transduction pathway as well as modulating cytoskeleton function. Although APC is expressed by Schwann cells, the role that it plays in these cells and in the myelination of the peripheral nervous system (PNS) is unknown. Therefore, we used the Cre-lox approach to generate a mouse model in which APC expression is specifically eliminated from Schwann cells. These mice display hindlimb weakness and impaired axonal conduction in sciatic nerves. Detailed morphological analyses revealed that APC loss delays radial axonal sorting and PNS myelination. Furthermore, APC loss delays Schwann cell differentiation *in vivo*, which correlates with persistent activation of the Wnt signaling pathway and results in perturbed extension of Schwann cell processes and disrupted lamellipodia formation. In addition, APC-deficient Schwann cells display a transient diminution of proliferative capacity. Our data indicate that APC is required by Schwann cells for their timely differentiation to mature, myelinating cells and plays a crucial role in radial axonal sorting and PNS myelination.

**KEY WORDS: Schwann cells, Radial axonal sorting, PNS, Adenomatous polyposis coli, Wnt signaling**

## INTRODUCTION

During the radial axonal sorting process, which starts around birth in the rodent PNS, immature Schwann cells extend cytoplasmic processes to axon bundles and initiate the sorting of axons based on size. Schwann cells establish a one-to-one ratio with large-caliber axons and thereafter myelinate them. Small-caliber axons remain as bundles (known as Remak bundles) and are surrounded by non-myelinating Schwann cells. Axonal sorting is a highly regulated process that is controlled by concerted signals intrinsic and extrinsic to Schwann cells. Extrinsic signals originate either from the axons and include the signal transducer proteins neuregulin 1 (Nrg1) (Birchmeier and Nave, 2008) and Notch1 (Woodhoo et al., 2009) or from the extracellular matrix, which includes proteins such as laminins, β1 integrin (Itgb1) (Feltri et al., 2002) and Rac1 (Nodari et al., 2007). Schwann cell-intrinsic signals include the transcription factors β-catenin (Ctnnb1) (Grigoryan et al., 2013), Sox10 (Finzsch et al., 2010) and Sox2 (Le et al., 2005).

Adenomatous polyposis coli (APC) is a member of the β-catenin destruction complex that mediates the degradation of β-catenin and thereby is involved in the Wnt signaling pathway (Nathke, 2006). Loss of APC leads to persistent activation of β-catenin, which results in tumor formation in the colon (Nathke, 2006). In addition to its involvement in the Wnt signaling pathway, APC is localized to membrane-protrusive areas and tips, where it binds to the plus end of microtubules and interacts with multiple RNAs and proteins to form APC-containing ribonucleoprotein complexes (Mili et al., 2008; Reilein and Nelson, 2005). APC was also shown to interact with actin and is believed to control actin-based cell protrusion (Okada et al., 2010). The binding between APC and the cytoskeleton stabilizes the cytoskeleton, prevents its collapse (Kroboth et al., 2007) and enables the cell to extend processes (Votin et al., 2005). Interaction of APC with the cytoskeleton is, at least in part, independent of Wnt signaling (Harris and Nelson, 2010). Owing to the role that APC plays in the regulation of β-catenin and because of its interaction with the cytoskeleton, we decided to investigate APC function in radial sorting and myelination of the PNS.

To examine the specific role of APC in Schwann cells we used a *P0-Cre* (P0 is also known as Mpz) transgenic mouse line (Feltri et al., 1999) in combination with mice containing a conditional *Apc* allele (Shibata et al., 1997) to generate mice in which APC is specifically eliminated from Schwann cells. Histological analysis revealed that loss of APC in Schwann cells delays radial axonal sorting and myelination in the sciatic nerve of the $Apc^{lox/lox}$;*P0-Cre* mice. Furthermore, APC-deficient Schwann cells displayed aberrant process formation *in vitro* and a transient proliferative deficiency and delayed differentiation *in vivo*. Taken together, our data indicate that APC is required by Schwann cells for their timely differentiation to mature, myelinating cells and plays an essential role in the extension of Schwann cell processes, radial axonal sorting and PNS myelination.

## RESULTS

### Hindlimb weakness and impaired axonal conduction in the PNS of the $Apc^{lox/lox}$;*P0-Cre* mice

Schwann cell-specific conditional *Apc* knockout mice ($Apc^{lox/lox}$;*P0-Cre*) were generated by mating mice carrying an *Apc* allele in which exon 14 was flanked by *loxP* sites (Shibata et al., 1997) with *P0-Cre* transgenic mice (Feltri et al., 1999). Sciatic nerve-specific excision was verified using PCR primers that exclusively recognize the excised allele (Fig. 1A). In order to study the timing of *Apc* excision, we quantified the levels of the excised allele in the sciatic nerve at different time points. We found that the excised allele is present at high levels as early as postnatal day 1 (P1) and continues to be detected approximately at the same levels at P60, the latest time

[1]Department of Neurology, Center for Peripheral Neuropathy, University of Chicago, Chicago, IL 60637, USA. [2]Stanford University School of Medicine, Department of Neurobiology, Fairchild Building Room D235, 299 Campus Drive, Stanford, CA 94305-5125, USA. [3]UNC Neuroscience Center and the Department of Cell and Molecular Physiology, University of North Carolina School of Medicine, Chapel Hill, NC 27599, USA.

*Author for correspondence (bpopko@uchicago.edu)

B.P., 0000-0001-9948-2553

**Received 29 January 2016; Accepted 9 May 2016**

Development (2016) 143, 2356-2366 doi:10.1242/dev.135913

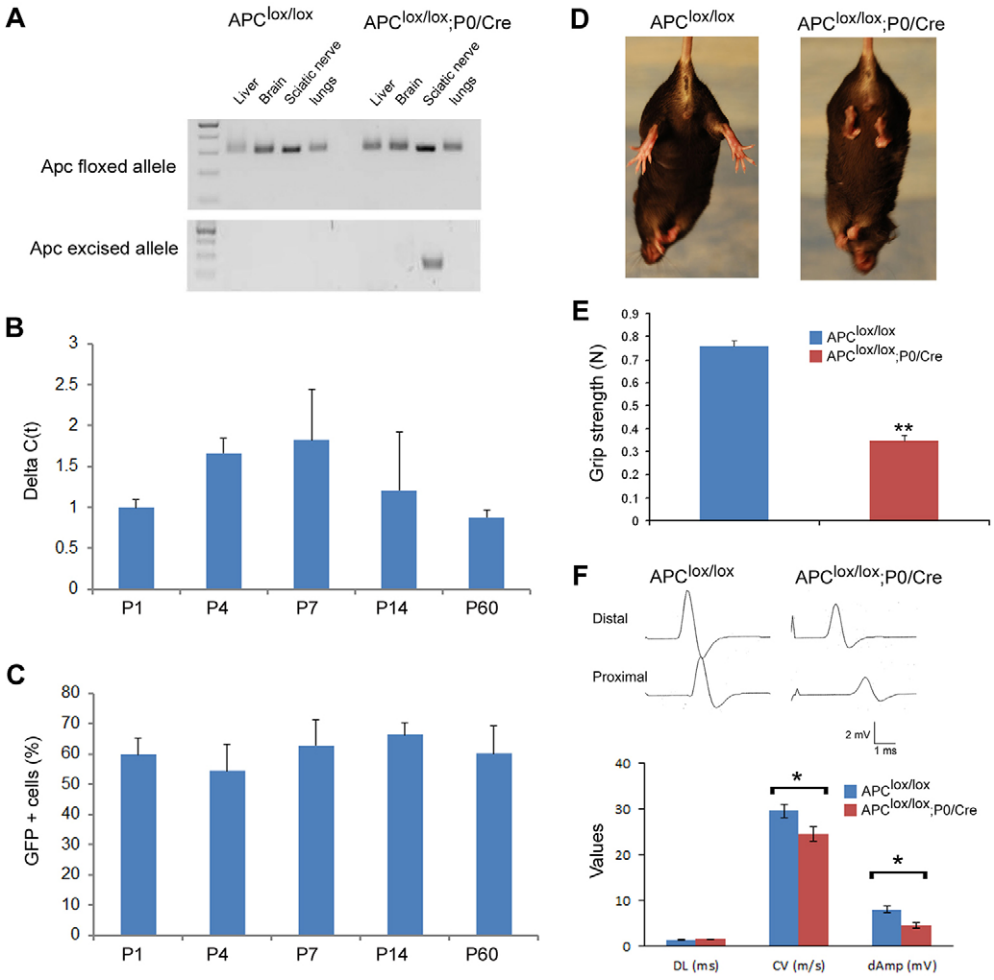


**Fig. 1. *Apc*$^{lox/lox}$*;P0-Cre* mice exhibit hindlimb weakness and impaired axonal conduction in the sciatic nerve.** (A) Excision of *Apc* exon 14 was verified in sciatic nerves of P7 *Apc*$^{lox/lox}$*;P0-Cre* mice using genomic DNA and primers that recognize the excised allele only: both the *Apc*$^{lox/lox}$*;P0-Cre* and *Apc*$^{lox/lox}$ (used as control) carry the Apc exon 14 *loxP*-flanked allele (top panel), whereas the excised allele can be detected in sciatic nerve of *Apc*$^{lox/lox}$*;P0-Cre* mice only (bottom panel). (B) The excised *Apc* allele was also detected at different time points by quantitative PCR analysis on genomic DNA extracted from sciatic nerves of *Apc*$^{lox/lox}$*;P0-Cre* and *Apc*$^{lox/lox}$ (control) mice. *Il2* was used as an internal control gene for normalization. (C) In order to study the recombination efficiency of the *P0-Cre* line, we generated a *ROSA26-stop-EYFP;P0-Cre* reporter line. YFP$^{+}$ cells were labeled in sciatic nerves of *ROSA26-stop-EYFP;P0-Cre* mice at different ages with an anti-GFP antibody and the percentage of DAPI$^{+}$ cells expressing the YPF reporter gene protein was quantified. (D) *Apc*$^{lox/lox}$*;P0-Cre* mice exhibit hindlimb clenching when suspended by the tail, a common neuropathic phenotype. (E) *Apc*$^{lox/lox}$*;P0-Cre* mice also suffer from hindlimb weakness as detected by the grip strength assay. (F) The conduction velocity and the amplitude of compound muscle action potential were both significantly reduced in sciatic nerves of the *Apc*$^{lox/lox}$*;P0-Cre* mice. For detection of the excised allele, three to four animals were taken per each time point. The excised allele was not detected in the *Apc*$^{lox/lox}$ mice at any time point. For reporter line assay, sciatic nerves from three to four animals were harvested per each time point. No YFP-positive cells were detected in control littermate *ROSA26-stop-EYFP* mice (Cre negative) at any time point. For grip strength assay: *Apc*$^{lox/lox}$, $n$=11 mice and *Apc*$^{lox/lox}$*;P0-Cre*, $n$=16 mice at P60. For electrophysiological studies: *Apc*$^{lox/lox}$, $n$=7 mice and *Apc*$^{lox/lox}$*;P0-Cre*, $n$=6 mice at P60. DL, distal latency; CV, conduction velocity; dAmp, distal amplitude. *$P$<0.05, **$P$<0.001.

point that we examined (Fig. 1B). We also crossed the reporter mouse line *ROSA26-stop-EYFP* (Srinivas et al., 2001) with the *P0-Cre* mice and found reporter gene expression in approximately 60% of the sciatic nerve cells at all time points examined (Fig. 1C and Fig. S1).

*Apc*$^{lox/lox}$*;P0-Cre* mice exhibit hindlimb clenching when suspended by the tail, a common indication of neurological dysfunction (Golan et al., 2013; Novak et al., 2011; Porrello et al., 2014) (Fig. 1D), and they also suffer from hindlimb weakness as detected by grip strength analysis (Fig. 1E). In order to examine peripheral nerve function, mutant and wild-type animals were subjected to electrophysiological examination, which showed that conduction velocity and the compound muscle action potential amplitude were both significantly reduced in sciatic nerves of the *Apc* $^{lox/lox}$*;P0-Cre* mice (Fig. 1F).

## APC loss in Schwann cells disrupts PNS myelination

The reduced conduction velocity detected in the sciatic nerves of the *Apc*$^{lox/lox}$*;P0-Cre* mice suggests the presence of myelination defects in these animals. Therefore, we examined the morphology of sciatic nerves of *Apc*$^{lox/lox}$*;P0-Cre* and control mice. The number of myelinated fibers was significantly reduced in the sciatic nerve of the *Apc*$^{lox/lox}$*;P0-Cre* mice at postnatal days (P) 1, 4 and 7 compared with controls (Fig. 2A,E). Nevertheless, the number of myelinated fibers was similar between the two genotypes at P14 – the peak of the PNS myelination – suggesting that the myelination process is delayed in the *Apc*$^{lox/lox}$*;P0-Cre* mutant animals during the early postnatal period. We also observed occasional abnormal polyaxonal myelination in which individual thin myelin sheaths wrapped multiple small-caliber axons, which affected ∼12% of the axons of

Development (2016) 143, 2356-2366 doi:10.1242/dev.135913

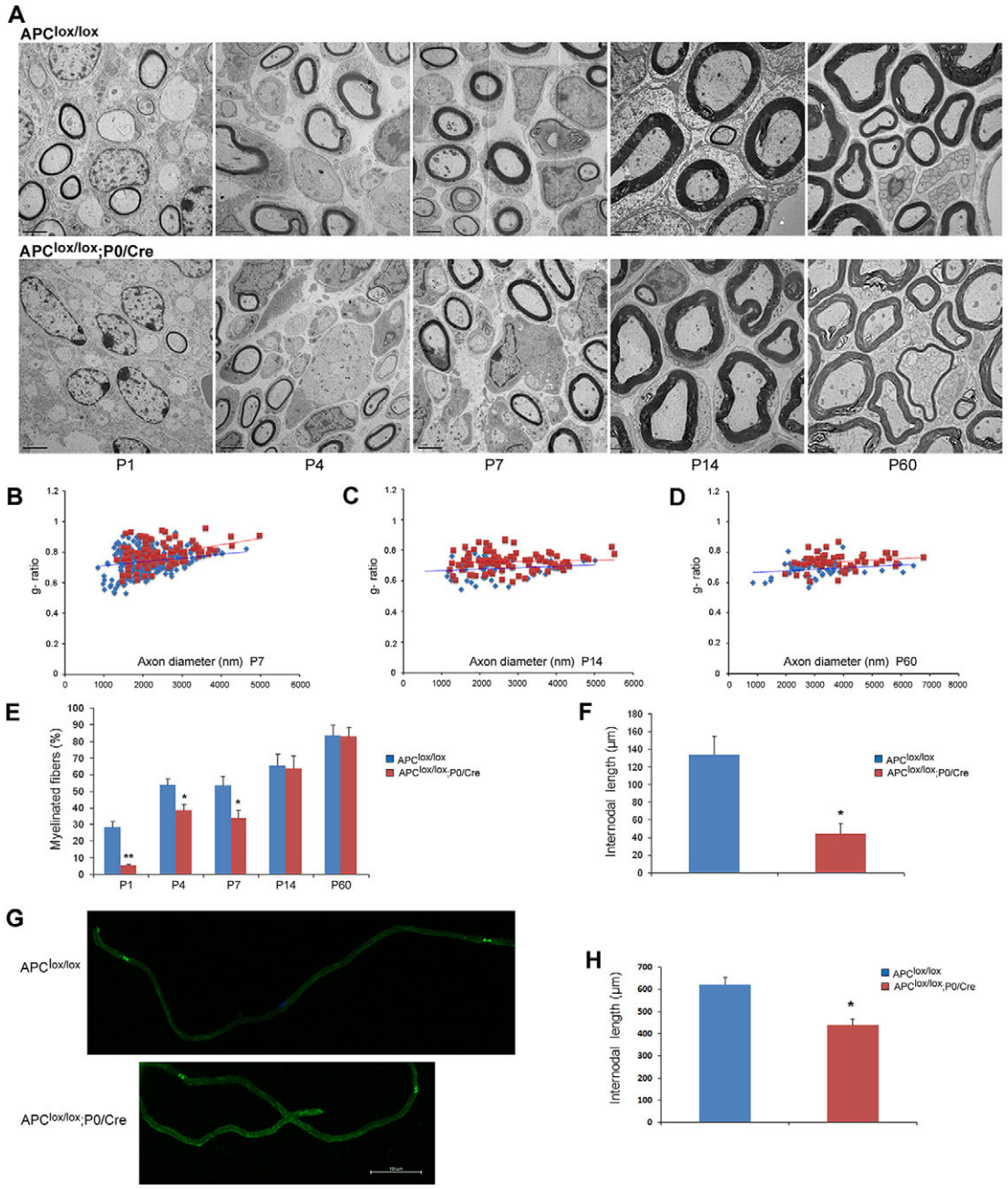


**Fig. 2. Loss of APC disrupts PNS myelination.** The sciatic nerves of *Apc*$^{lox/lox}$*;P0-Cre* mutant and *Apc*$^{lox/lox}$ control mice were analyzed by electron microscopy (EM). (A) The number of myelinated fibers is significantly reduced in the sciatic nerves of the *Apc*$^{lox/lox}$*;P0-Cre* mice at P1, P4 and P7 compared with control mice. Scale bars: 2 µm. (B-D) *Apc*$^{lox/lox}$*;P0-Cre* mice have a thinner myelin (higher g-ratio) compared with controls at P7 (B), P14 (C) and P60 (D). At P7, the mean g-ratio in the *Apc*$^{lox/lox}$*;P0-Cre* mice was 0.782 (±0.004) compared with 0.73 (±0.007) in the *Apc*$^{lox/lox}$ mice, $^{**}P<0.001$. At P14, the mean g-ratio in the *Apc*$^{lox/lox}$*;P0-Cre* mice was 0.72 (±0.006) compared to 0.68 (±0.009) in the *Apc*$^{lox/lox}$ mice, $^{**}P<0.001$. At P60, the mean g-ratio in the *Apc*$^{lox/lox}$*;P0-Cre* mice was 0.73 (±0.007) compared to 0.68 (±0.007) in the *Apc*$^{lox/lox}$ mice, $^{**}P<0.001$. (E) *Apc*$^{lox/lox}$*;P0-Cre* sciatic nerve contained fewer myelinated axons at P1, P4 and P7. $^{*}P<0.05$, $^{**}P<0.001$. (F) Three-dimensional EM images were acquired from sciatic nerve serial sections of *Apc*$^{lox/lox}$*;P0-Cre* and *Apc*$^{lox/lox}$ (control) mice at P7, and individual nerve fibers were traced and analyzed in reconstructed EM images of both genotypes. The *Apc*$^{lox/lox}$*;P0-Cre* sciatic nerve contained much shorter internodes compared with controls. (G) Sciatic nerves of *Apc*$^{lox/lox}$*;P0-Cre* and *Apc*$^{lox/lox}$ control mice at P60 were teased and immunolabeled for paranodin/Caspr, a marker of paranodal junctions to measure internodal length in adulthood. (H) Quantitative analysis showed that the *Apc*$^{lox/lox}$*;P0-Cre* sciatic nerves contained much shorter internodes compared with controls. For EM analysis, at least three mice were taken for each time point, per genotype. For g-ratio analysis, at least 50 axons from at least three mice per genotype were analyzed. The number of internodes analyzed *in vivo* in P7 animals was: *Apc*$^{lox/lox}$, *n*=9; *Apc*$^{lox/lox}$*;P0-Cre*, *n*=8; $^{*}P<0.05$. The number of internodes analyzed in teased fibers of P60 animals was: *Apc*$^{lox/lox}$, *n*=46; *Apc*$^{lox/lox}$*;P0-Cre*, *n*=37; $^{*}P<0.05$. Internodes from at least three mice per genotype were analyzed.

these mice at P60 (Fig. 2A; higher magnification in Fig. S2). This finding may be due to abnormal axonal sorting in the *Apc*$^{lox/lox}$*;P0-Cre* sciatic nerves. In addition, *Apc*$^{lox/lox}$*;P0-Cre* sciatic nerves contained axons with thinner myelin (higher g-ratios) compared with controls at P7-P60 (Fig. 2B-D), strongly indicating that APC loss results in PNS hypomyelination.

Development (2016) 143, 2356-2366 doi:10.1242/dev.135913

Since we saw profound hypomyelination in *Apc*$^{lox/lox}$*;P0-Cre* mice compared with control mice at P7, we performed a detailed morphometric analysis of the P7 sciatic nerves. We used 3DEM (serial blockface scanning EM) to further analyze the myelin sheath abnormalities observed in the PNS of the *Apc*$^{lox/lox}$*;P0-Cre* mice at P7. EM images of serial sections were acquired from sciatic nerves of *Apc*$^{lox/lox}$*;P0-Cre* and *Apc*$^{lox/lox}$ (control) mice and individual fibers were traced and analyzed in both genotypes. We found that the mutant sciatic nerve contained fewer myelinated axons compared with controls, confirming that the mutant sciatic nerve is significantly hypomyelinated. The results are presented in Movies 1-4. Three-dimensional reconstruction of the serial EM images showed that mutant sciatic nerves contained ∼3 times shorter internodes at P7 (Fig. 2F) regardless of the axon diameter (Fig. S3). This phenotype persists to adulthood, since shorter internodes were also detected in teased sciatic nerve fibers stained for the paranodal marker Caspr (Menegoz et al., 1997) at P60 (Fig. 2G,H). The reduced myelin thickness and shorter internodes of the *Apc*$^{lox/lox}$*;P0-Cre* mice probably explains the electrophysiological abnormalities (Fig. 1F) found in these animals.

### APC loss in Schwann cells disrupts radial axonal sorting

APC loss in Schwann cells appears to disrupt radial axonal sorting, since we observed abnormally large bundles of axons in the sciatic nerves of the *Apc*$^{lox/lox}$*;P0-Cre* mice (Fig. 3B) that were absent in *Apc*$^{lox/lox}$ control mice (Fig. 3A). The mutant axonal bundles were approximately three times larger than the bundles found in control mice at P1, P4, P7 and P14 (Fig. 3E), suggesting that the axonal sorting process was disrupted in the mutant animals during the early postnatal period. The axon bundles of the mutant mice were larger because they contained large- and small-caliber axons in contrast to the bundles of the control mice that contained only small-caliber axons (Fig. 3F and G). The simultaneous presence of large- and small-caliber axons in the mutant axonal bundles further indicates

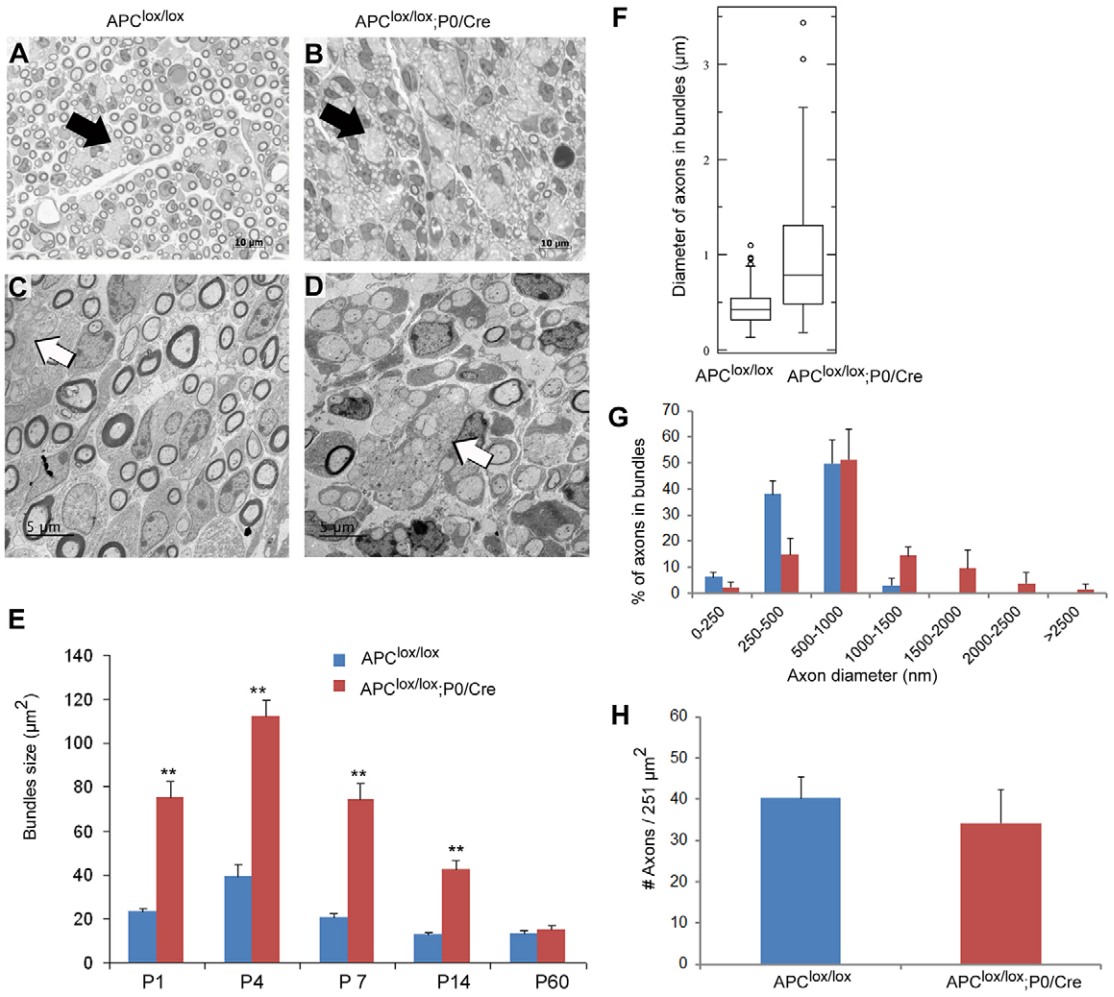


**Fig. 3. APC loss disrupts the radial axonal sorting process in the PNS.** The sciatic nerves of *Apc*$^{lox/lox}$*;P0-Cre* and control *Apc*$^{lox/lox}$ mice were analyzed morphometrically on Toluidine Blue-stained semi-thin sections (A,B) and by EM (C,D). (A,B) The sciatic nerves of the *Apc*$^{lox/lox}$*;P0-Cre* mice contained large bundles of axons compared with control mice. Black arrows indicate bundles of axons. Scale bars: 10 µm. (C,D) *Apc*$^{lox/lox}$*;P0-Cre* bundles of axons contained large- and small-caliber axons (D) in contrast to the bundles found in control mice (C) that contained small-caliber axons only. White arrows indicate bundles of axons. Scale bars: 5 µm. (E) The large bundles of axons were ∼3 times larger than the bundles of the control mice at P1, P4, P7 and P14. (F) *Apc*$^{lox/lox}$*;P0-Cre* large bundles of axons contained large- and small-caliber axons in contrast to the bundles found in control mice. Box plots show the 25–75% range (box) and 2.5–97.5% range (whiskers). (G) The bundles of unsorted axons in the *Apc*$^{lox/lox}$*;P0-Cre* mice contained a higher percentage of large-caliber axons (diameter >1 µm). (H) The density of the axons was not statistically different between *Apc*$^{lox/lox}$*;P0-Cre* mice and the control mice at P7. The images in A-D were taken from P7 mice. Axon bundles were analyzed from at least three mice per genotype. Axon diameter was analyzed from at least three mice per genotype at P7. ***P*<0.001. Large-caliber axons were defined here as axons with diameter of 1 µm and above. Low-caliber axons were defined here as axons with diameter less than 1 µm.

Development (2016) 143, 2356-2366 doi:10.1242/dev.135913

that the radial axonal sorting process was disrupted in the *Apc*$^{lox/lox}$*;P0-Cre* mice. The delayed sorting and hypomyelination observed at P7 was not accompanied by axonal loss because the density of axons was not significantly different between the mutant and control mice at P7 (Fig. 3H).

### APC loss in Schwann cells results in delayed differentiation

To determine if the delay in PNS myelination in *Apc*$^{lox/lox}$*;P0-Cre* mice was correlated with an alteration in Schwann cell development, we examined the expression of Schwann cell lineage markers in P7 sciatic nerves. Scip (also known as Pou3f1) and Krox20 (also known as Egr2) are key transcriptional factors in the Schwann cell differentiation program. Scip is a marker of premyelinating Schwann cells (Bermingham et al., 1996) and Krox20 is a marker of myelinating Schwann cells (Topilko et al., 1994). We found increased numbers of premyelinating Schwann cells labeled for Scip (Fig. 4A,B) and reduced numbers of myelinating Schwann cells labeled for Krox20 in P7 sciatic nerves of the *Apc*$^{lox/lox}$*;P0-Cre* mice compared with controls (Fig. 4C and D), suggesting that the differentiation of Schwann cells into myelin-forming cells is delayed. We also examined cell division in the mutant sciatic nerves using the proliferation marker Ki67. Although there was no difference in the number of Ki67$^{+}$ cells (Fig. 4E,F) or the total number of Schwann cell nuclei (Fig. S4) present in the mutant and control nerves at P7, when examined at P1, a reduction in Ki67$^{+}$ cells was detected in the *Apc*$^{lox/lox}$*;P0-Cre* sciatic nerve, suggesting aberrant Schwann cell proliferation in the absence of APC (Fig. S4).

In order to further characterize the delayed differentiation of the mutant Schwann cells, we analyzed the expression of several genes that are known to be differentially expressed along the Schwann cell lineage in sciatic nerves (Eccleston et al., 1987; Jessen and Mirsky, 2005; Woodhoo et al., 2009). We found that APC loss results in the upregulation of genes specifically expressed in immature, premyelinating Schwann cells such as *Scip*, *Sox2* and *Galc* (Fig. 5A) and downregulation of myelin-specific genes expressed in mature myelinating Schwann cells (Fig. 5B).

APC loss might dysregulate the Wnt/β-catenin signaling pathway in Schwann cells that has been shown to be crucial for PNS myelination (Grigoryan et al., 2013). APC is a member of the β-catenin destruction complex that mediates the degradation of β-catenin. In the absence of APC, β-catenin does not undergo degradation resulting in constant activation of the Wnt signaling pathway (Nathke, 2006). Consistent with this, we found that expression of the Wnt signaling target genes *Axin2*, *Myc* and *Lef*

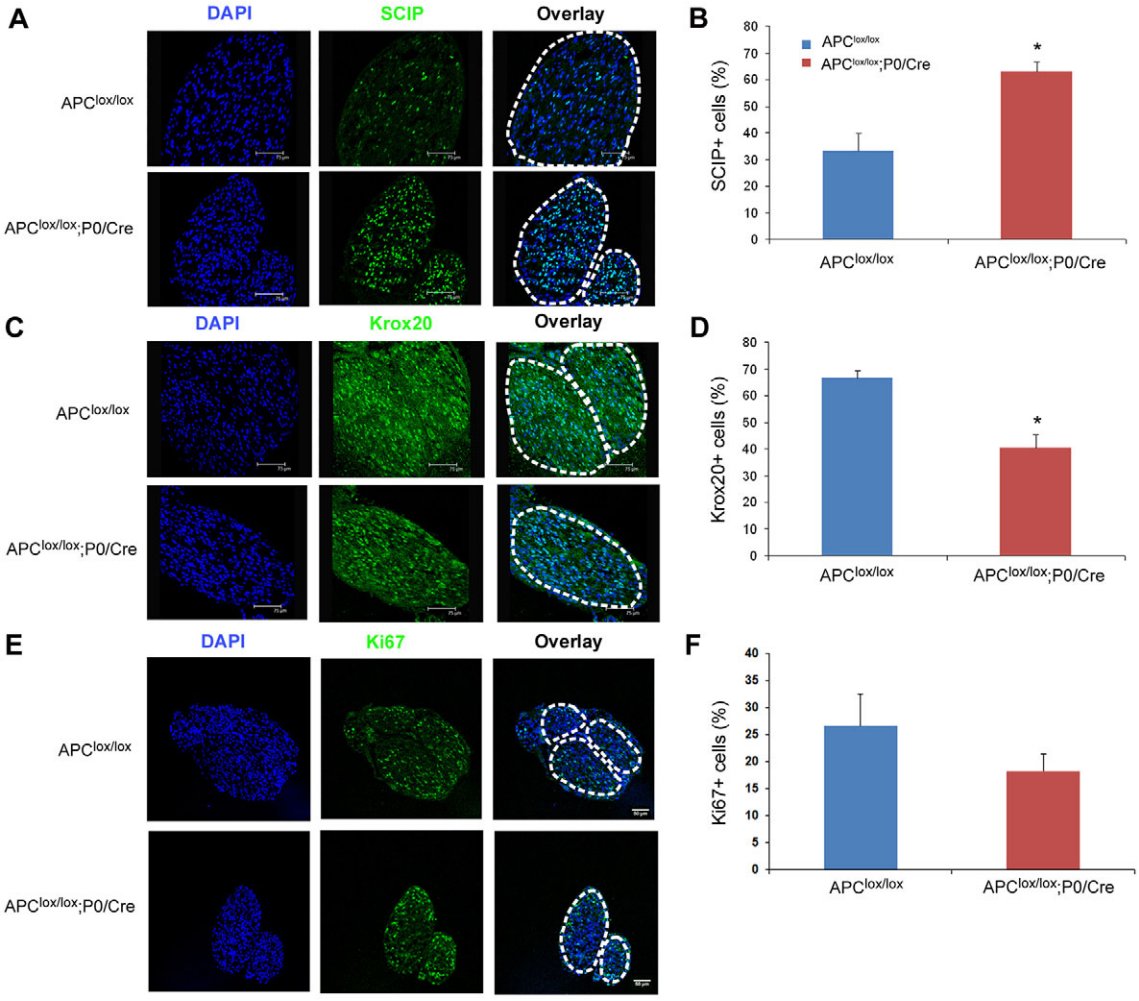


**Fig. 4. Delayed differentiation of APC-deficient Schwann cells.** (A) *Apc*$^{lox/lox}$*;P0-Cre* sciatic nerve has increased numbers of premyelinating Scip$^{+}$ Schwann cells. (C) *Apc*$^{lox/lox}$*;P0-Cre* sciatic nerve has reduced numbers of myelinating Krox20$^{+}$ Schwann cells. (E) Ablation of APC results in a slight, non-statistically significant, reduction in cell proliferation. Graphs in B,D,F show quantitative analysis of data in A,C,E, respectively. *Apc*$^{lox/lox}$, *n*=4 mice; *Apc*$^{lox/lox}$*;P0-Cre*, *n*=3 mice at P7; **P*<0.005.

Development (2016) 143, 2356-2366 doi:10.1242/dev.135913

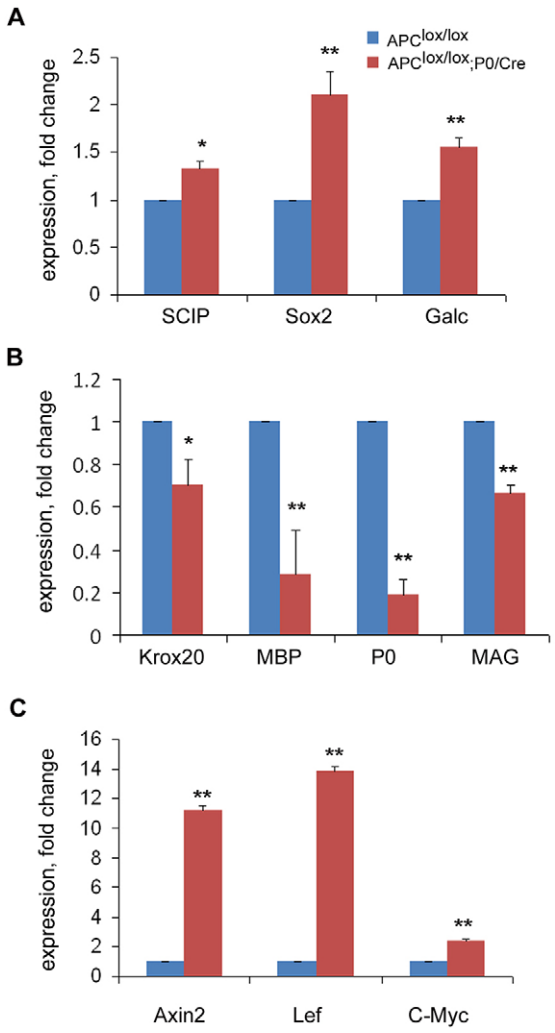


**Fig. 5. Loss of APC results in upregulation of Wnt signaling target genes and delayed differentiation of Schwann cells.** (A) Expression of immature Schwann cell genes *Scip*, *Sox2* and *Galc* is upregulated. (B) The expression of mature myelinating Schwann cell genes *Krox20*, *Mbp*, *P0* and *Mag* is downregulated in *Apc*$^{lox/lox}$*;P0-Cre* sciatic nerves compared with controls at P7. (C) Expression of the Wnt signaling target genes *Axin2*, *Myc* and *Lef* is upregulated in the sciatic nerves of *Apc*$^{lox/lox}$*;P0-Cre* mice compared with controls at P7. *Apc*$^{lox/lox}$, $n$=3 mice; *Apc*$^{lox/lox}$*;P0-Cre*, $n$=3 mice. *$P$<0.05, **$P$<0.001.

were all upregulated in the sciatic nerves of the *Apc*$^{lox/lox}$*;P0-Cre* mice at P7, indicating that loss of APC activates the Wnt signaling pathway in APC-deficient Schwann cells (Fig. 5C). This data indicates that the role of APC in controlling the Wnt signaling pathway potentially contributes an essential function in the differentiation program of Schwann cells.

### APC loss in Schwann cells leads to perturbed extension of processes and increased lamellipodia formation

It was previously shown that APC forms a complex with actin (Okada et al., 2010) and is also localized to the plus end of microtubules, where it interacts with the cytoskeleton (Nathke, 2006). In agreement with these observations, primary Schwann cells in culture displayed APC staining in processes, where it colocalized with F-actin and α-tubulin, and in lamellipodia, where it colocalized with F-actin (Fig. S5). Prior reports indicated that the interaction of APC with the cytoskeleton may regulate cell process formation and extension in radial glia, astrocytes and neurons (Imura et al., 2010; Wang et al., 2011; Yokota et al., 2009). In order to test the possibility that APC also controls process extension in Schwann cells, we traced and measured the length of these cells in 3DEM serial sciatic nerve sections of *Apc*$^{lox/lox}$*;P0-Cre* and *Apc*$^{lox/lox}$ control mice. We found that mutant Schwann cells *in vivo* were on average much shorter compared with control cells (Fig. 6A). Since the Schwann cells in the control mice were very long and many of them expanded over the length of the 3DEM sections, the number of Schwann cells available for this analysis was limited. Therefore, we cultured primary Schwann cells from sciatic nerves of *Apc*$^{lox/lox}$*;P0-Cre* and *Apc*$^{lox/lox}$ control mice using an immunopanning technique (Brosius Lutz, 2014). Using primary Schwann cell cultures stained for the Schwann cell marker S100, we detected shorter Schwann cell processes in the *Apc*$^{lox/lox}$*;P0-Cre* mice (Fig. 6B,C).

It has been shown previously that activation of Wnt signaling results in increased lamellipodia formation and an increased number of processes in Schwann cells (Grigoryan et al., 2013). Similarly, we found that APC loss leads to increased numbers of lamellipodia in *Apc*$^{lox/lox}$*;P0-Cre* mutant Schwann cells (Fig. 6D) when plated on laminin. In order to assess whether APC ablation affects lamellipodia formation through a laminin/β1 integrin-dependent mechanism, we plated the cells on the β1 integrin-independent substrate vitronectin. This assay showed, however, that the change in lamellipodia formation observed in the APC-ablated cells was not β1 integrin dependent since a similar increase was observed in cells plated on vitronectin (Fig. S6). The APC mutant Schwann cells showed normal numbers of cell processes (Fig. 6E).

### Role of the Wnt signaling pathway in lamellipodia formation in Schwann cells

The proteins APC, GSK3β and Axin2 compose the β-catenin destruction complex that mediates the degradation of β-catenin (Nathke, 2006). In the absence of APC, this complex disassembles, β-catenin does not undergo degradation and the Wnt signaling pathway remains activated (Nathke, 2006). In order to assess whether the lamellipodia-related phenotype observed in the APC-ablated cells is dependent on the β-catenin destruction complex, we modulated Wnt signaling with small molecules that target either GSK3β or Axin2. To activate Wnt signaling we used CHIR99021, which is a potent inhibitor of GSK3β, and to inhibit Wnt signaling, we used XAV939, which is an inhibitor of tankyrase 1 and 2 (TNKS), the enzymes responsible for the degradation of the axin-GSK3β complex (Huang et al., 2009). By inhibiting TNKS activity, XAV939 thereby promotes the degradation of β-catenin, resulting in inhibition of the Wnt signaling pathway (Fig. 7). In wild-type Schwann cells, activation of Wnt signaling with CHIR99021 resulted in increased lamellipodia formation and inhibition of the pathway with XAV939 resulted in reduced lamellipodia formation (Fig. 7C). In the absence of β-catenin inhibition, we speculated that the APC-ablated cells would be insensitive to the modulation of Wnt signaling. Consistent with this hypothesis, lamellipodia formation in the APC mutant Schwann cells was resistant to both Wnt pathway activation and inhibition (Fig. 7C). Moreover, neither drug had an effect on the extension of processes in wild-type or APC mutant Schwann cells, suggesting that this phenotype is not dependent on the Wnt signaling pathway (Fig. 7B,D).

## DISCUSSION

In the present study, we used the well characterized *P0-Cre* transgenic mouse line (Feltri et al., 1999) to conditionally ablate APC expression from Schwann cells. The resultant *Apc*$^{lox/lox}$*;*

Development (2016) 143, 2356-2366 doi:10.1242/dev.135913

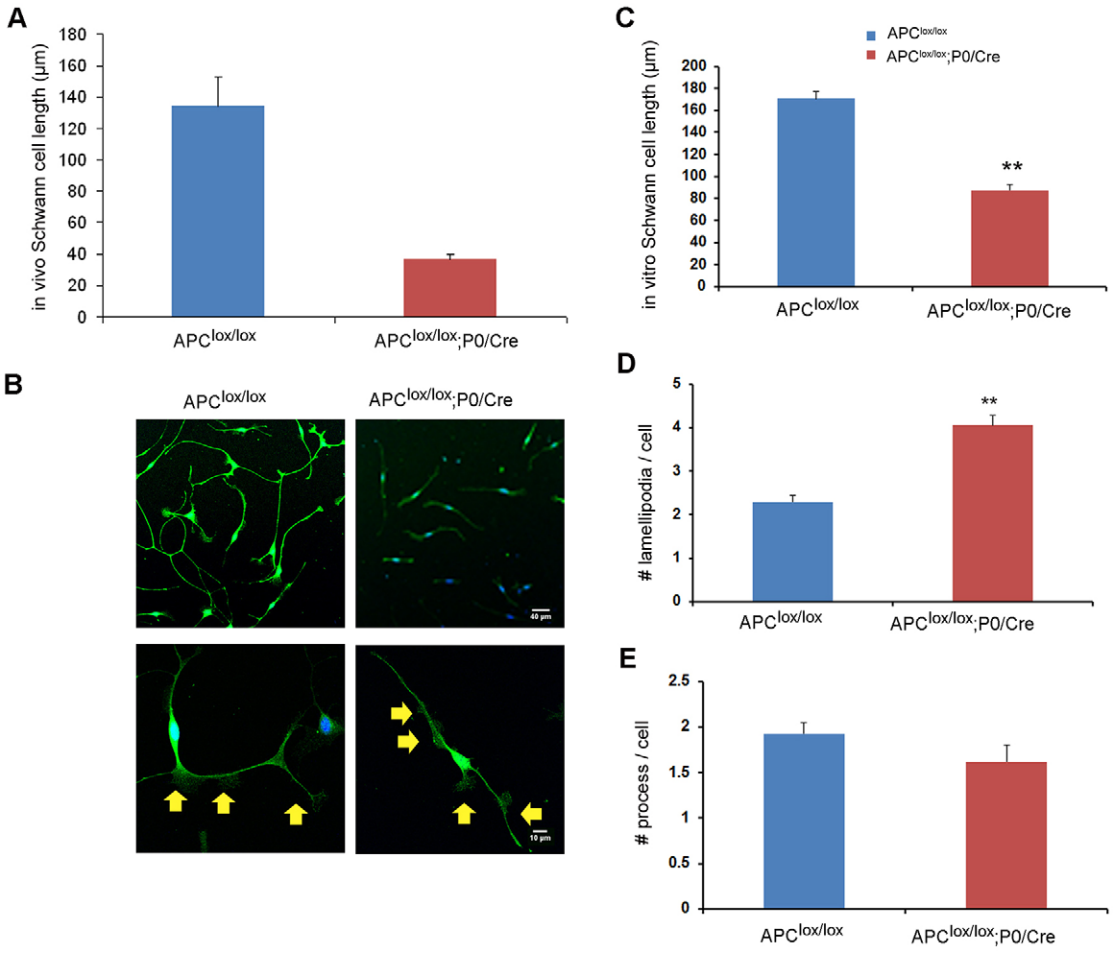


**Fig. 6. Loss of APC results in perturbed Schwann cell process extension and lamellipodia formation.** 3DEM images of serial sections were acquired from sciatic nerves of *Apc*$^{lox/lox}$*;P0-Cre* and *Apc*$^{lox/lox}$ (control) mice at P7 and individual Schwann cells traced and analyzed in both genotypes. (A) Detailed analysis of a single Schwann cell in the 3DEM images of sciatic nerves revealed the presence of shorter cell processes in *Apc*$^{lox/lox}$*;P0-Cre* mice. (B) Primary Schwann cells were cultured and stained for S100, a Schwann cell marker. The Schwann cells derived from the *Apc*$^{lox/lox}$*;P0-Cre* sciatic nerves were much shorter (quantified results in C). Increased numbers of lamellipodia per cell were detected in the Schwann cells derived from the *Apc*$^{lox/lox}$*;P0-Cre* sciatic nerves (quantified results in D). Yellow arrows indicate lamellipodia. (E) No significant changes in the number of cell processes were found in the mutant cells compared with controls. Number of Schwann cells traced and analyzed *in vivo* in the sciatic nerves: *Apc*$^{lox/lox}$, *n*=5; *Apc*$^{lox/lox}$*;P0-Cre*, *n*=27; ***P*<0.001. Number of cells analyzed *in vitro* (primary culture): *Apc*$^{lox/lox}$, *n*=414; *Apc*$^{lox/lox}$*;P0-Cre*, *n*=469; ***P*<0.001.

*P0-Cre* animals exhibit hindlimb weakness and impaired axonal conduction in the sciatic nerve. We showed that radial axonal sorting and PNS myelination are delayed in these animals. Our data suggest that the delayed sorting and myelination observed in the *Apc*$^{lox/lox}$*;P0-Cre* animals are likely to be the result of delayed Schwann cell differentiation. Our data also suggest that APC loss affects lamellipodia formation and process extension in Schwann cells during PNS myelination.

The role of APC in CNS myelination has been investigated; APC was shown to be important for CNS myelination and remyelination (Fancy et al., 2009). APC is expressed transiently in oligodendrocyte lineage cells during development, where it regulates formation of processes (Lang et al., 2013). Ablation of APC from oligodendrocytes altered the expression of genes involved in actin and microtubule polymerization, as well as genes involved in the generation of the cytoskeleton (Lang et al., 2013). The mechanism by which APC controls CNS myelination is complex and may be attributed to aberrant regulation of Wnt signaling and/or to abnormal expression of cytoskeletal proteins in the oligodendrocytes that lack APC (Lang et al., 2013).

Since APC is expressed in Schwann cells, we speculated that it might also be important for PNS myelination. Previous studies have conditionally inactivated APC expression in the developing neural crest, which resulted in apoptosis of cephalic and cardiac neural crest cells at about 11.5 days post coitum, resulting in craniofacial and cardiac anomalies at birth (Hasegawa et al., 2002). Nevertheless, the Cre driver line that was used in this study activated *loxP* recombination in Schwann cells as well as neuronal cells and ventral craniofacial mesenchyme (Yamauchi et al., 1999). Therefore, the specific role of APC in Schwann cells has not been addressed. We showed here that loss of APC in Schwann cells delays differentiation, resulting in disrupted radial axonal sorting and diminished PNS myelination during the early postnatal period. This delay in radial axonal sorting and PNS myelination results in a persistent PNS neuropathy as displayed by hindlimb weakness and electrophysiological abnormalities in adult animals. This neuropathy is probably the result of the shorter internodes and reduced myelin thickness observed in these animals.

APC is a member of the β-catenin destruction complex that mediates the degradation of β-catenin. In the absence of APC,

Development (2016) 143, 2356-2366 doi:10.1242/dev.135913

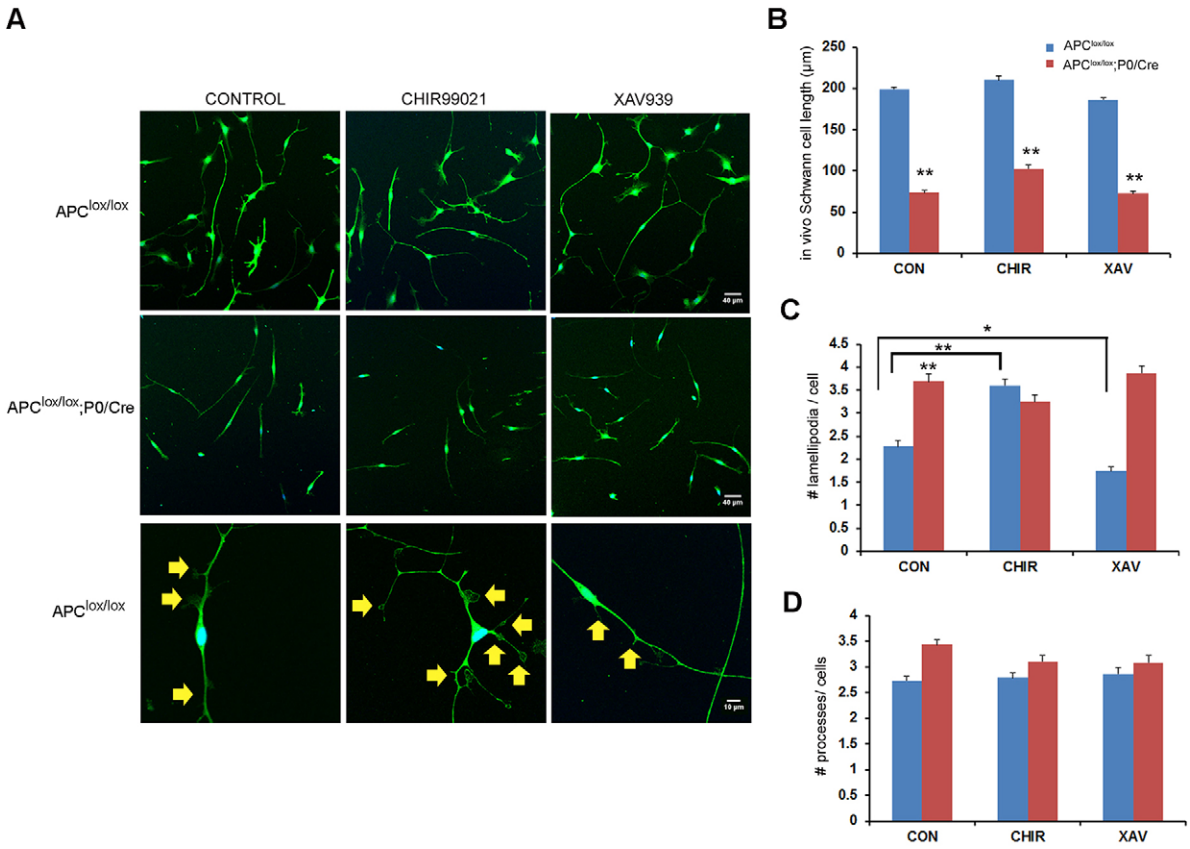


**Fig. 7. Role of the Wnt signaling pathway in lamellipodia formation in Schwann cells.** (A) Primary Schwann cells were cultured on laminin-coated plates in the presence of either the Wnt signaling activator CHIR99021 or the Wnt signaling inhibitor XAV939 or with DMSO (used as control; CON). The cells were fixed and stained for S100, a Schwann cell marker. (B) The Schwann cells derived from *Apc$^{lox/lox}$;P0-Cre* sciatic nerves were shorter, regardless of treatment. (C) Lamellipodia formation was increased in the *Apc$^{lox/lox}$*-derived cells upon CHIR99021 treatment, and decreased upon XAV939 treatment. The treatments did not affect lamellipodia formation in the cells derived from the *Apc$^{lox/lox}$;P0-Cre* mice. (D) No significant changes were detected in the number of processes per cell in either genotype. Number of cells analyzed *in vitro* (primary culture): DMSO control: *Apc$^{lox/lox}$*, *n*=736; *Apc$^{lox/lox}$;P0-Cre*, *n*=534; CHIR99021: *Apc$^{lox/lox}$*, *n*=625; *Apc$^{lox/lox}$;P0-Cre*, *n*=552; XAV939: *Apc$^{lox/lox}$*, *n*=558; *Apc$^{lox/lox}$;P0-Cre*, *n*=684; **P*<0.05, ***P*<0.001. Yellow arrows indicate lamellipodia.

β-catenin does not undergo degradation, resulting in persistent activation of the Wnt signaling pathway (Nathke, 2006). Accordingly, we showed that loss of APC activates the Wnt signaling pathway in *Apc$^{lox/lox}$;P0-Cre* sciatic nerves, resulting in upregulation of genes specifically expressed in immature premyelinating Schwann cells and downregulation of myelin-specific gene expression.

Activating the Wnt signaling pathway in Schwann cells by distinct approaches results in similar phenotypes; the β-catenin gain-of-function (GOF) mutation (Grigoryan et al., 2013) and APC depletion in our study both result in upregulation of genes specifically expressed in premyelinating Schwann cells and delayed myelination. Both the β-catenin GOF mutants and the *Apc$^{lox/lox}$;P0-Cre* mutants showed upregulation of *Sox2* gene expression, which is an inhibitor of Schwann cell differentiation and myelination (Le et al., 2005). Sox2 has been shown to downregulate Krox20 expression (Le et al., 2005), which could explain the reduction in Krox20$^{+}$ cells present in the *Apc$^{lox/lox}$;P0-Cre* mice. Therefore, we suggest that APC controls Schwann cell differentiation and PNS myelination soon after birth by inhibiting the Wnt signaling pathway in Schwann cells.

Nevertheless, despite very similar effects on myelination and on Schwann cell differentiation, the β-catenin GOF and the APC depletion mutations appear to have opposite effects on axonal sorting: the β-catenin GOF mutation accelerates the radial axonal sorting process, whereas the APC ablation described here delays axonal sorting despite the activation of the Wnt signaling pathway. Our observations indicate that APC might affect radial axonal sorting through a Wnt-independent mechanism: by using a pharmacological approach, we demonstrated that the abnormal extension of processes in APC-ablated Schwann cells is likely to be the result of a Wnt signaling-independent mechanism whereas the aberrant lamellipodia formation observed in these cells appears to depend on Wnt signaling. Proper lamellipodia formation is important for radial axonal sorting and for PNS myelination (Nodari et al., 2007), therefore its aberrant formation may explain, at least in part, the sorting and myelination defects in the *Apc$^{lox/lox}$;P0-Cre* mice. In addition, during PNS development, radial axonal sorting is contingent on normal extension of processes by Schwann cells (Feltri et al., 2016). Therefore, the inability of the APC-ablated Schwann cells to extend normal processes, which was observed *in vivo* and *in vitro*, may explain the sorting failure that occurs in the *Apc$^{lox/lox}$;P0-Cre* mice.

In the PNS, proteins involved in the Wnt signaling pathway are expressed by both neurons and Schwann cells. In Schwann cells, Wnt signaling activity is highest at E15.5-E17.5 and declines subsequently (Grigoryan et al., 2013). Our data suggest that the Wnt signaling pathway plays a fundamental role in Schwann cell maturation and PNS myelination, as suggested previously (Grigoryan et al., 2013; Jacob et al., 2011).

Development (2016) 143, 2356-2366 doi:10.1242/dev.135913

In addition, we observed a reduction in Schwann cell proliferation in P1 animals in the absence of APC expression. This result was surprising in that APC was identified as a tumor suppressor and in most situations, its inactivation results in uncontrolled cellular proliferation. Nevertheless, the inactivation of APC in CNS radial glial cells also results in a reduced proliferative capacity of these cells (Yokota et al., 2009). Despite the reduced Schwann cell proliferation observed in the newborn mice in the absence of APC, Schwann cell proliferation and the total number of cells present in the mutant sciatic nerve recovered to normal levels by P7. The extent to which this transient Schwann cell proliferative defect contributes to the overall mutant phenotype remains to be determined.

The work presented here reveals a novel role of APC in PNS myelination. Our genetic and pharmacological results indicate that APC controls Schwann cell process extension, lamellipodia formation and differentiation through Wnt signaling-dependent as well as Wnt signaling-independent mechanisms. Therefore, our study expands knowledge of the molecular mechanisms controlling radial axonal sorting and PNS myelination by Schwann cells, which could support our efforts to better understand PNS disorders.

## MATERIALS AND METHODS

### Mice

Mice were housed and studied according to the University of Chicago's Animal Care and Use Committee (IACUC) guidelines. PNS-specific conditional knockout *Apc* mice (*Apc*$^{lox/lox}$*;P0-Cre*) were generated by mating mice carrying an *Apc* allele in which exon 14 is flanked by *loxP* sites (Shibata et al., 1997) with the *P0-Cre* transgenic mouse line (Feltri et al., 1999). Littermate *Apc*$^{lox/lox}$ mice served as controls. Mice were genotyped by PCR analysis of tail genomic DNA using the primers P3 (5′-GTTCT-GTATCATGGAAAGATAGGTGGTC-3′) and P4 (5′-CACTCAAAACG-CTTTTGAGGGTTGATTC-3′). The excised allele was detected using primers P5 (5′-GAGTACGGGGTCTCTGTCTCAGTGAA-3′) and P3 (Shibata et al., 1997). The *P0-Cre* reporter line was generated by mating *ROSA26-stop-EYFP* mice (Srinivas et al., 2001) with the *P0-Cre* transgenic mouse line (Feltri et al., 1999).

### Grip strength analysis

We measured muscle strength in mouse hindlimbs using a computerized grip strength meter (model # 0167-005L) from Columbus Instruments (Columbus, OH). Two trials of 10 measurements per trial were performed for each animal with a 2 min resting period between each measurement. The average force (newton, N) was calculated for each group.

### Electrophysiology

Electrophysiology was performed with a Nicolet Viking Quest Laptop System (VikQuest Port 4ch-7) from Nicolet Biomedical (Madison, WI). Recording needle electrodes were placed subcutaneously in the footpad. Supramaximal stimulation of sciatic nerves was performed with a 0.1-0.2 ms pulse, stimulating distally at the ankles and proximally at the sciatic notch with needle electrodes. Latencies, conduction velocities and amplitudes of compound muscle action potentials were measured. Results from stimulation of bilateral sciatic nerves were averaged for each animal, with *n* representing the number of animals in each group.

### Primary Schwann cell cultures

Schwann cells were isolated from *Apc*$^{lox/lox}$*;P0-Cre* and *Apc*$^{lox/lox}$ mouse sciatic nerves using a sequential immunopanning protocol (Brosius Lutz, 2014). Briefly, 30 sciatic nerves from P7 pups were dissected and enzymatically dissociated with a collagenase and dispase mixture at 37°C. After enzymatic dissociation and gentle trituration, the single-cell suspension was sequentially incubated on dishes coated with antibodies against CD45 (macrophage depletion), Thy1.2 (fibroblast depletion) and O4 (Schwann cell selection). O4$^{+}$ Schwann cells were trypsinized from the O4-coated panning plate and seeded onto poly-D-lysine and laminin-coated 12 mm glass coverslips. In some experiments, the cells were seeded onto poly-D-lysine, vitronectin or bovine serum albumin (BSA)-coated plates.

### Immunohistochemistry

Animals were anesthetized by intraperitoneal injection with avertin (0.5 mg/g) and the sciatic nerve tissues were harvested and snap-frozen in isopentane precooled in liquid nitrogen. Cross-sections were cut from the fresh frozen tissue, fixed for 10 min in 4% paraformaldehyde, washed in PBS and subjected to immunostaining. The antibodies used were against Krox20 (Covance, PRB-236P, 1:250), Scip (Santa Cruz Biotechnology, sc11661, 1:250), Ki67 (eBiosciences, A15, 1:250), GFP (Invitrogen, A21311, 1:500), Cspr (Abcam, ab34151, 1:500), S100b (Dako, z0311, 1:500), APC (Santa Cruz Biotechnology, sc896, 1:150) and α-tubulin (Invitrogen, A11126, 1:250). Phalloidin was used for F-actin labeling (Thermo Fisher, A12381, 1:50). Confocal images of the sciatic nerves were generated on a Leica SP2-AOBS laser scanning microscope (Germany) equipped with an argon laser that excites at 488 nm and a helium/neon laser that excites at 543 nm, using a 20× or 40×/1.4 objective and a pinhole size of 1.0 airy disk units.

### Histological and morphometric analysis

*Apc*$^{lox/lox}$*;P0-Cre* or littermate *Apc*$^{lox/lox}$ mice (served as controls) were perfused intracardially through the left ventricle with saline for 2 min, followed by perfusion with a solution of 2.5% glutaraldehyde and 4% paraformaldehyde in a 0.1 M sodium cacodylate buffer. Sciatic nerves were harvested and post-fixed in the same fixative at 4°C for 2 weeks and sciatic nerve samples were embedded in epoxy resin. Ultrathin cross-sections of the sciatic nerve were cut, double stained with uranyl acetate and lead citrate and observed on a Philips CM 10 electron microscope. G-ratios were calculated from the sciatic nerves of three or four mice for each genotype. The g-ratios were calculated as axon diameter/fiber diameter as described previously (Auer, 1994).

### Serial blockface scanning EM (3DEM)

For 3DEM analysis, P7 *Apc*$^{lox/lox}$*;P0-Cre* or littermate *Apc*$^{lox/lox}$ mice (served as control) were perfused with 2.5% glutaraldehyde and 4% paraformaldehyde in a 0.1 M sodium cacodylate buffer and the sciatic nerves were dissected, postfixed in the same fixative and submitted to Renovo Neural Inc. for 3DEM analysis. Briefly, 500 µm tissue was stained with heavy metals, embedded in Epon resin and mounted onto pins (detailed protocol available from Renovo Neural). Serial blockface micrographs (analogous to serial sectioning) were obtained using a Zeiss Sigma VP scanning electron microscope equipped with a Gatan 3View in-chamber ultramicrotome. Series of approximately 250 images were acquired at 2.25 kV with a resolution of 10 nm per pixel and 100 nm per section, resulting in a field analysis of 204.8 µm ($x$)×61.44 µm ($y$)×25 µm ($z$). Images were registered and resized as necessary using ImageJ/FIJI software (http://fiji.sc/). For Schwann cell length analysis, we traced and measured the length of Schwann cells containing a classic Remak bundle, Schwann cells containing large diameter axons (one or more) and Schwann cells containing very small diameter axon bundles.

### Quantitative real-time PCR

Total RNA was extracted from 26-32 sciatic nerves of P7 *Apc*$^{lox/lox}$*;P0-Cre* or littermate *Apc*$^{lox/lox}$ mice (served as controls) using the TRIzol reagent (Invitrogen). RNA integrity was verified using Agilent chip (Agilent Technologies). cDNA was synthesized using iScript cDNA synthesis kit (Bio-Rad) according to the manufacturer's instructions. Real-time qRT-PCR was performed using iQ SYBER Green Supermix (Bio-Rad) according to the manufacturer's instructions. *Gapdh* was used as internal control gene for normalization. The following set of primers were used: *Myc* forward, 5′-TTGGAAACCCCGCAGACAG-3′ and *Myc* reverse, 5′-GCTGTACG-GAGTCGTAGTCG-3′; *Axin2* forward, 5′-AAGCCCCATAGTGCCCAA-AG-3′ and *Axin2* reverse, 5′-GGGTCCTGGGTAAATGGGTG-3′; *Lef1* forward, 5′-ATGCACGTGAAGCCTCAACA-3′ and *Lef1* reverse, 5′-AG-CTGCACTCTCCTTTAGCG-3′; *Mbp* forward, 5′-ACACGAGAACTAC-CCATTATGGC-3′ and *Mbp* reverse, 5′-CCAGCTAAATCTGCTGAGG-GA; *Galc* forward, 5′-GCCTACGTGCTAGACGACTC-3′ and *Galc*

Development (2016) 143, 2356-2366 doi:10.1242/dev.135913

reverse, 5′-AGAACGATAGGGCTCTGGGT-3′; *P0* forward, 5′-ACCTC-TCAGGTCACGCTCTA-3′ and *P0* reverse, 5′-CATGGCACTGAGCCT-TCTCTG-3′; *Mag* forward, 5′-TTTGGACGTCAAGTACCCCC-3′ and *Mag* reverse, 5′-GGTACAGGCTCTTGGCAACT-3′.

For quantification of the *Apc*-excised allele we used genomic DNA extracted from sciatic nerves using Red Extract Kit (Sigma). The excised allele was amplified using SYBR Green Extract-N-Amp qPCR kit (Sigma) according to the manufacturer's instructions and the *Apc* gene P4 and P3 primers. The *Il2* gene was also amplified as an internal control gene for normalization using the primers 5′-CTAGGCCACAGAATTGAAAG-ATCT-3′ (forward) and 5′-GTAGGTGGAAATTCTAGCATCATCC-3′ (reverse).

## Statistical analysis

Statistical significance was determined using one-way ANOVA for electrophysiological measurements, Wilcoxon signed-rank test for intermodal length, and Student's *t*-test for all the rest. Differences were considered to be statistically significant if $P<0.05$. All results are expressed as the mean±s.e.m.

### Acknowledgements

We thank Dr Laura Feltri and Dr Lawrence Wrabetz for providing the *P0-Cre* mice. We thank Erdong Liu, Gloria Wright, Ani Solanki and Yimei Chen for skilful technical assistance and Andrew Roholt (Renovo Neural) for assistance with serial blockface scanning electron microscopy analysis.

### Competing interests

The authors declare no competing or financial interests.

### Author contributions

B.E.: designed research, performed research, analyzed data, wrote the paper; M.T. and B.S.: performed research, analyzed data; R.B.K. and D.D.: performed research; A.B.L., E.S.A. and B.A.B.: contributed unpublished reagents/analytic tools; B.P.: designed research, analyzed data, wrote the paper.

### Funding

This work was funded by the National Institutes of Health [R01 NS067550 to B.P.]. Deposited in PMC for release after 12 months.

### Supplementary information

Supplementary information available online at
http://dev.biologists.org/lookup/doi/10.1242/dev.135913.supplemental

### References

**Auer, R. N.** (1994). Automated nerve fibre size and myelin sheath measurement using microcomputer-based digital image analysis: theory, method and results. *J. Neurosci. Methods* **51**, 229-238.

**Bermingham, J. R., Jr, Scherer, S. S., O'Connell, S., Arroyo, E., Kalla, K. A., Powell, F. L. and Rosenfeld, M. G.** (1996). Tst-1/Oct-6/SCIP regulates a unique step in peripheral myelination and is required for normal respiration. *Genes Dev.* **10**, 1751-1762.

**Birchmeier, C. and Nave, K.-A.** (2008). Neuregulin-1, a key axonal signal that drives Schwann cell growth and differentiation. *Glia* **56**, 1491-1497.

**Brosius Lutz, A.** (2014). Purification of Schwann cells from the neonatal and injured adult mouse peripheral nerve. In *Purifying and Culturing Neural Cells: A Laboratory Manual* (ed. B. S. Ben and A. Barres), pp. 177-188. Cold Spring Harbor Laboratory Press (in print).

**Eccleston, P. A., Mirsky, R., Jessen, K. R., Sommer, I. and Schachner, M.** (1987). Postnatal development of rat peripheral nerves: an immunohistochemical study of membrane lipids common to non-myelin forming Schwann cells, myelin forming Schwann cells and oligodendrocytes. *Brain Res. Dev Brain Res.* **432**, 249-256.

**Fancy, S. P. J., Baranzini, S. E., Zhao, C., Yuk, D.-I., Irvine, K.-A., Kaing, S., Sanai, N., Franklin, R. J. M. and Rowitch, D. H.** (2009). Dysregulation of the Wnt pathway inhibits timely myelination and remyelination in the mammalian CNS. *Genes Dev.* **23**, 1571-1585.

**Feltri, M. L., D'Antonio, M., Previtali, S., Fasolini, M., Messing, A. and Wrabetz, L.** (1999). P0-Cre transgenic mice for inactivation of adhesion molecules in Schwann cells. *Ann. N. Y. Acad. Sci.* **883**, 116-123.

**Feltri, M. L., Graus Porta, D., Previtali, S. C., Nodari, A., Migliavacca, B., Cassetti, A., Littlewood-Evans, A., Reichardt, L. F., Messing, A., Quattrini, A. et al.** (2002). Conditional disruption of beta 1 integrin in Schwann cells impedes interactions with axons. *J. Cell Biol.* **156**, 199-210.

**Feltri, M. L., Poitelon, Y. and Previtali, S. C.** (2016). How Schwann cells sort axons: new concepts. *Neuroscientist.* **22**, 252-265.

**Finzsch, M., Schreiner, S., Kichko, T., Reeh, P., Tamm, E. R., Bösl, M. R., Meijer, D. and Wegner, M.** (2010). Sox10 is required for Schwann cell identity and progression beyond the immature Schwann cell stage. *J. Cell Biol.* **189**, 701-712.

**Golan, N., Kartvelishvily, E., Spiegel, I., Salomon, D., Sabanay, H., Rechav, K., Vainshtein, A., Frechter, S., Maik-Rachline, G., Eshed-Eisenbach, Y. et al.** (2013). Genetic deletion of Cadm4 results in myelin abnormalities resembling Charcot-Marie-Tooth neuropathy. *J. Neurosci.* **33**, 10950-10961.

**Grigoryan, T., Stein, S., Qi, J., Wende, H., Garratt, A. N., Nave, K.-A., Birchmeier, C. and Birchmeier, W.** (2013). Wnt/Rspondin/beta-catenin signals control axonal sorting and lineage progression in Schwann cell development. *Proc. Natl. Acad. Sci. USA* **110**, 18174-18179.

**Harris, E. S. and Nelson, W. J.** (2010). Adenomatous polyposis coli regulates endothelial cell migration independent of roles in beta-catenin signaling and cell-cell adhesion. *Mol. Biol. Cell* **21**, 2611-2623.

**Hasegawa, S., Sato, T., Akazawa, H., Okada, H., Maeno, A., Ito, M., Sugitani, Y., Shibata, H., Miyazaki, J.-I., Katsuki, M. et al.** (2002). Apoptosis in neural crest cells by functional loss of APC tumor suppressor gene. *Proc. Natl. Acad. Sci. USA* **99**, 297-302.

**Huang, S.-M. A., Mishina, Y. M., Liu, S., Cheung, A., Stegmeier, F., Michaud, G. A., Charlat, O., Wiellette, E., Zhang, Y., Wiessner, S. et al.** (2009). Tankyrase inhibition stabilizes axin and antagonizes Wnt signalling. *Nature* **461**, 614-620.

**Imura, T., Wang, X., Noda, T., Sofroniew, M. V. and Fushiki, S.** (2010). Adenomatous polyposis coli is essential for both neuronal differentiation and maintenance of adult neural stem cells in subventricular zone and hippocampus. *Stem Cells* **28**, 2053-2064.

**Jacob, C., Christen, C. N., Pereira, J. A., Somandin, C., Baggiolini, A., Lötscher, P., Özcelik, M., Tricaud, N., Meijer, D., Yamaguchi, T. et al.** (2011). HDAC1 and HDAC2 control the transcriptional program of myelination and the survival of Schwann cells. *Nat. Neurosci.* **14**, 429-436.

**Jessen, K. R. and Mirsky, R.** (2005). The origin and development of glial cells in peripheral nerves. *Nat. Rev. Neurosci.* **6**, 671-682.

**Kroboth, K., Newton, I. P., Kita, K., Dikovskaya, D., Zumbrunn, J., Waterman-Storer, C. M. and Nathke, I. S.** (2007). Lack of adenomatous polyposis coli protein correlates with a decrease in cell migration and overall changes in microtubule stability. *Mol. Biol. Cell* **18**, 910-918.

**Lang, J., Maeda, Y., Bannerman, P., Xu, J., Horiuchi, M., Pleasure, D. and Guo, F.** (2013). Adenomatous polyposis coli regulates oligodendroglial development. *J. Neurosci.* **33**, 3113-3130.

**Le, N., Nagarajan, R., Wang, J. Y. T., Araki, T., Schmidt, R. E. and Milbrandt, J.** (2005). Analysis of congenital hypomyelinating Egr2Lo/Lo nerves identifies Sox2 as an inhibitor of Schwann cell differentiation and myelination. *Proc. Natl. Acad. Sci. USA* **102**, 2596-2601.

**Menegoz, M., Gaspar, P., Le Bert, M., Galvez, T., Burgaya, F., Palfrey, C., Ezan, P., Arnos, F. and Girault, J.-A.** (1997). Paranodin, a glycoprotein of neuronal paranodal membranes. *Neuron* **19**, 319-331.

**Mili, S., Moissoglu, K. and Macara, I. G.** (2008). Genome-wide screen reveals APC-associated RNAs enriched in cell protrusions. *Nature* **453**, 115-119.

**Nathke, I.** (2006). Cytoskeleton out of the cupboard: colon cancer and cytoskeletal changes induced by loss of APC. *Nat. Rev. Cancer* **6**, 967-974.

**Nodari, A., Zambroni, D., Quattrini, A., Court, F. A., D'Urso, A., Recchia, A., Tybulewicz, V. L. J., Wrabetz, L. and Feltri, M. L.** (2007). Beta1 integrin activates Rac1 in Schwann cells to generate radial lamellae during axonal sorting and myelination. *J. Cell Biol.* **177**, 1063-1075.

**Novak, N., Bar, V., Sabanay, H., Frechter, S., Jaegle, M., Snapper, S. B., Meijer, D. and Peles, E.** (2011). N-WASP is required for membrane wrapping and myelination by Schwann cells. *J. Cell Biol.* **192**, 243-250.

**Okada, K., Bartolini, F., Deaconescu, A. M., Moseley, J. B., Dogic, Z., Grigorieff, N., Gundersen, G. G. and Goode, B. L.** (2010). Adenomatous polyposis coli protein nucleates actin assembly and synergizes with the formin mDia1. *J. Cell Biol.* **189**, 1087-1096.

**Porrello, E., Rivellini, C., Dina, G., Triolo, D., Del Carro, U., Ungaro, D., Panattoni, M., Feltri, M. L., Wrabetz, L., Pardi, R. et al.** (2014). Jab1 regulates Schwann cell proliferation and axonal sorting through p27. *J. Exp. Med.* **211**, 29-43.

**Reilein, A. and Nelson, W. J.** (2005). APC is a component of an organizing template for cortical microtubule networks. *Nat. Cell Biol.* **7**, 463-473.

**Shibata, H., Toyama, K., Shioya, H., Ito, M., Hirota, M., Hasegawa, S., Matsumoto, H., Takano, H., Akiyama, T., Toyoshima, K. et al.** (1997). Rapid colorectal adenoma formation initiated by conditional targeting of the Apc gene. *Science* **278**, 120-123.

**Srinivas, S., Watanabe, T., Lin, C.-S., William, C. M., Tanabe, Y., Jessell, T. M. and Costantini, F.** (2001). Cre reporter strains produced by targeted insertion of EYFP and ECFP into the ROSA26 locus. *BMC Dev. Biol.* **1**, 4.

**Topilko, P., Schneider-Maunoury, S., Levi, G., Baron-Van Evercooren, A., Chennoufi, A. B. Y., Seitanidou, T., Babinet, C. and Charnay, P.** (1994). Krox-20 controls myelination in the peripheral nervous system. *Nature* **371**, 796-799.

Development (2016) 143, 2356-2366 doi:10.1242/dev.135913

**Votin, V., Nelson, W. J. and Barth, A. I. M.** (2005). Neurite outgrowth involves adenomatous polyposis coli protein and beta-catenin. *J. Cell Sci.* **118**, 5699-5708.

**Wang, X., Imura, T., Sofroniew, M. V. and Fushiki, S.** (2011). Loss of adenomatous polyposis coli in Bergmann glia disrupts their unique architecture and leads to cell nonautonomous neurodegeneration of cerebellar Purkinje neurons. *Glia* **59**, 857-868.

**Woodhoo, A., Alonso, M. B. D., Droggiti, A., Turmaine, M., D'Antonio, M., Parkinson, D. B., Wilton, D. K., Al-Shawi, R., Simons, P., Shen, J. et al.** (2009). Notch controls embryonic Schwann cell differentiation, postnatal myelination and adult plasticity. *Nat. Neurosci.* **12**, 839-847.

**Yamauchi, Y., Abe, K., Mantani, A., Hitoshi, Y., Suzuki, M., Osuzu, F., Kuratani, S. and Yamamura, K.-I.** (1999). A novel transgenic technique that allows specific marking of the neural crest cell lineage in mice. *Dev. Biol.* **212**, 191-203.

**Yokota, Y., Kim, W.-Y., Chen, Y., Wang, X., Stanco, A., Komuro, Y., Snider, W. and Anton, E. S.** (2009). The adenomatous polyposis coli protein is an essential regulator of radial glial polarity and construction of the cerebral cortex. *Neuron* **61**, 42-56.

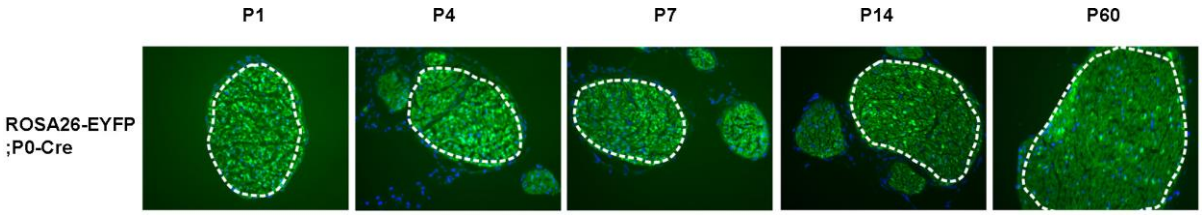


**Figure S1: Recombination efficiency of the ROSA26-stop-EYFP;*P0/Cre* reporter line**. In order to study the recombination efficiency of the *P0/Cre* driver line we generated ROSA26-stop-EYFP;*P0/Cre* reporter mice. YFP-positive cells were labeled in sciatic nerves of *ROSA26-stop-EYFP;P0/Cre* mice at different ages with an anti-GFP antibody. At least three mice were taken for each time point.

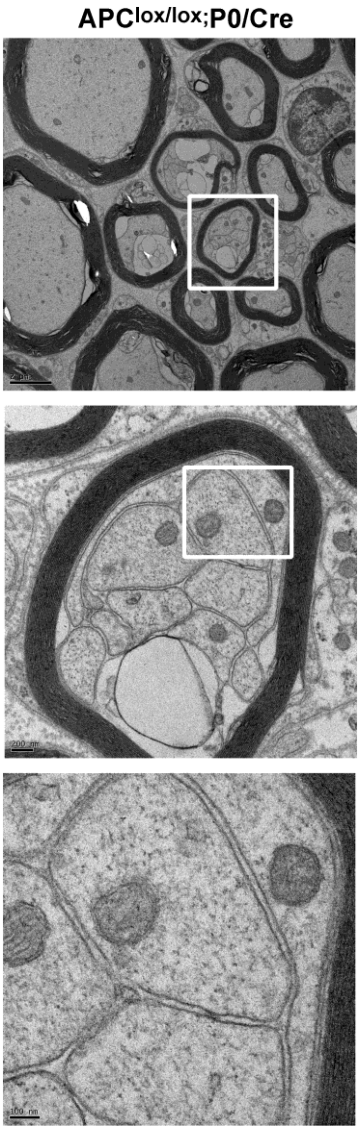


**Figure S2: Polyaxonal myelination in sciatic nerve of the *Apc$^{lox/lox}$;P0/Cre* mice**. Polyaxonal myelination was observed in the sciatic nerve of *Apc$^{ox/lox}$;P0/Cre* mice. As shown, thin myelin sheaths wrapped several small caliber axons. Scale bar represents 2 μm (upper panel), 200 nm (middle panel) or 100 nm (lower panel). Images were taken from an *Apc$^{lox/lox}$;P0/Cre* mouse at p60.

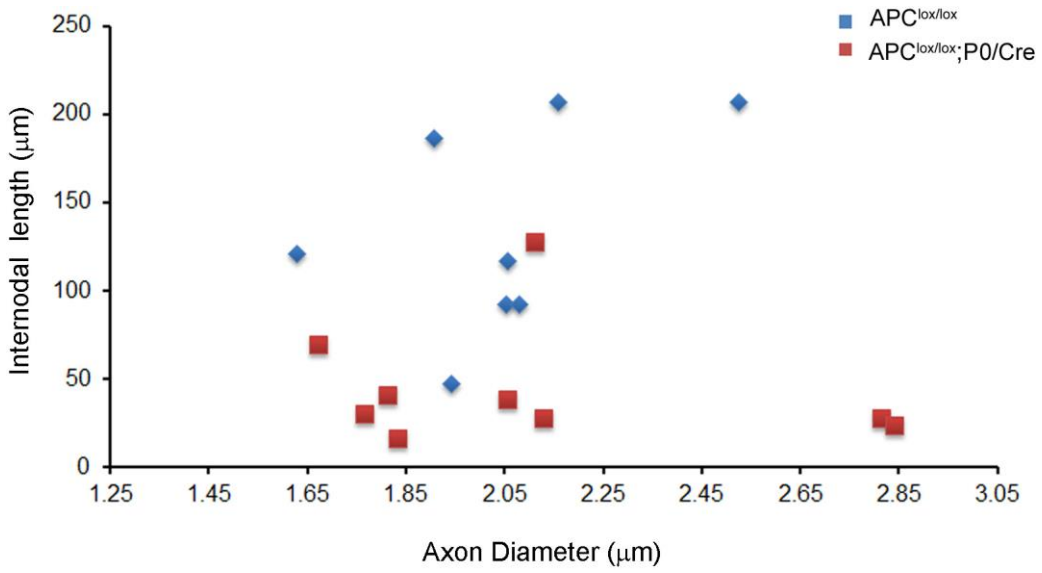


**Figure S3: The *Apc$^{lox/lox}$;P0/Cre* sciatic nerve contained much shorter internodes as compared to controls.** Three-dimensional EM images were acquired from sciatic nerve serial sections of *Apc$^{lox/lox}$;P0/Cre* and *Apc$^{lox/lox}$* (control) mice at P7, and individual nerve fibers were traced and analyzed in reconstructed EM images of both genotypes. It can be seen that the *Apc$^{lox/lox}$;P0/Cre* sciatic nerve contained much shorter internodes as compared to controls regardless of the axon diameter.

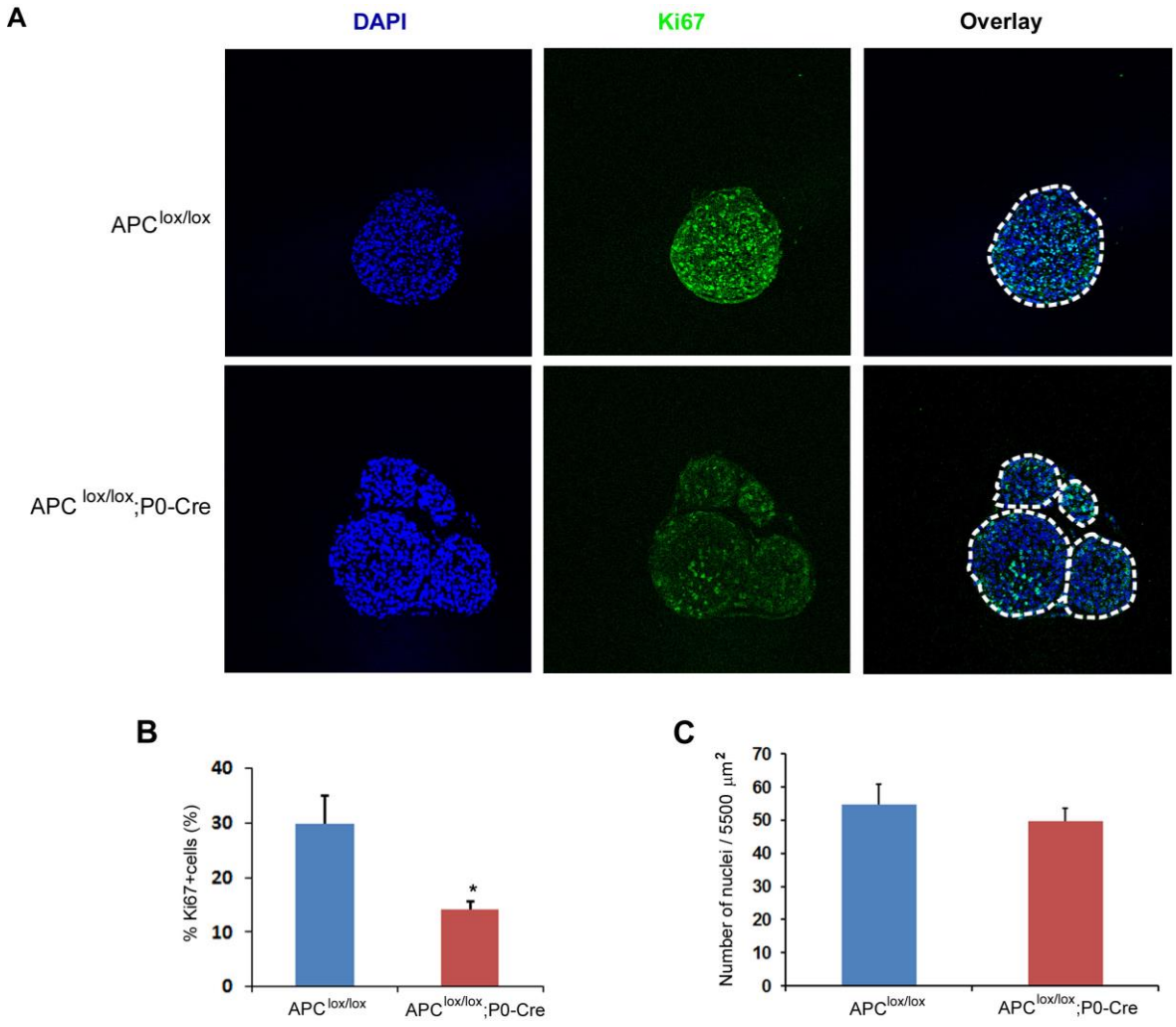


**Figure S4: The effect of APC Ablation on Schwann cell proliferation**. (A) *Apc$^{lox/lox}$;P0/Cre* sciatic nerves had reduced numbers of Ki67$^{+}$cells at P1. (B) Quantified results of Ki67$^{+}$cells at P1. N = 3 for both *Apc*$^{lox/lox}$ mice and *Apc*$^{lox/lox}$;P0/Cre mice, *p<0.005. (C) The sciatic nerves of *Apc$^{lox/lox}$;P0/Cre* and control *Apc$^{lox/lox}$* mice were analyzed morphometrically on toluidine blue-stained semi-thin sections at P7. The number of nuclei was not significantly different between the *Apc*$^{lox/lox}$ mice and *Apc*$^{lox/lox}$;P0/Cre mice at P7. N = 3 for both genotypes.

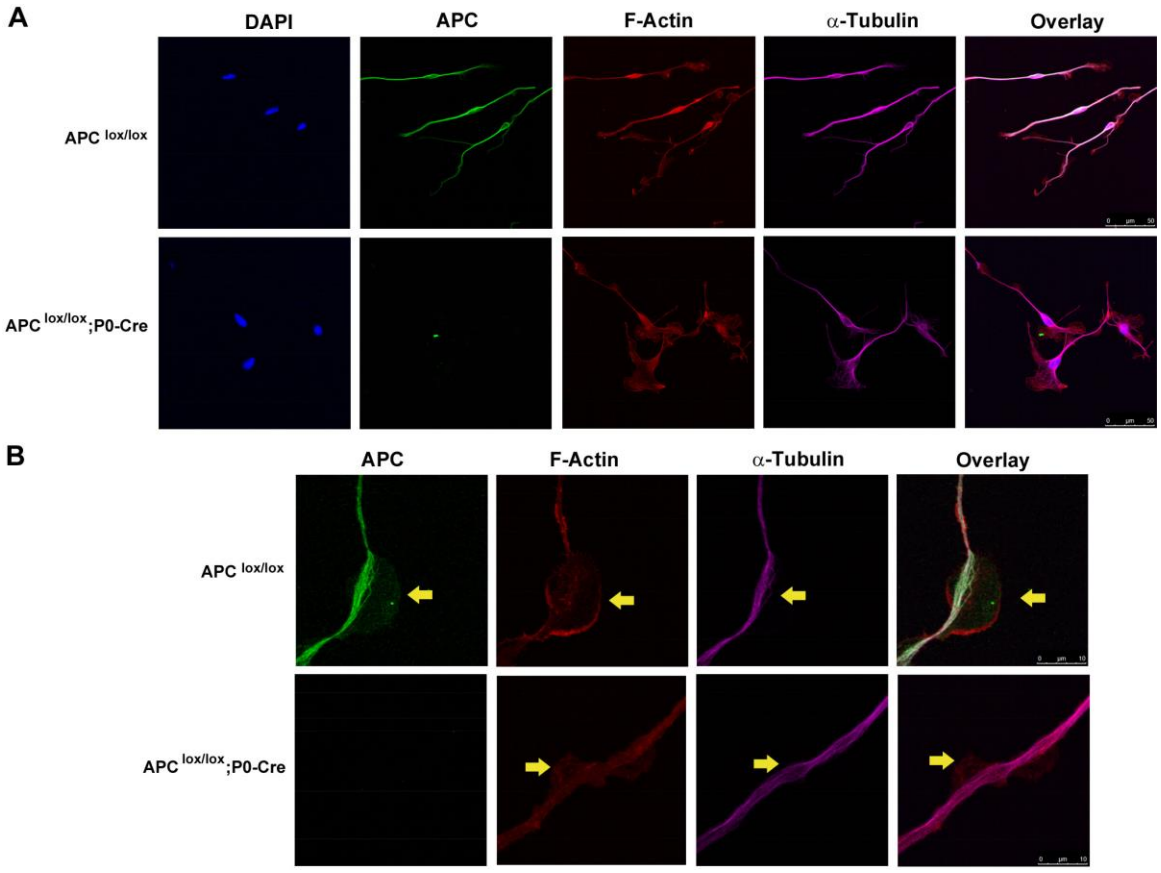


**Figure S5: APC is localized in the processes and in the lamellipodia of primary cultured Schwann cells.** Primary Schwann cells were cultured on laminin. The cells were fixed and stained with antibodies against APC and α-tubulin. The cells were stained also with phalloidin, which stains F-actin. (A) Our staining suggested that in primary cultured Schwann cells APC is localized in the processes where it colocalizes with F-actin and α-tubulin, and in the lamellipodia where it colocalizes with F-actin only. Yellow arrows mark lamellipodia. (B) Higher magnification. Bar represent 50 μm in (A) and 10 μm in (B).

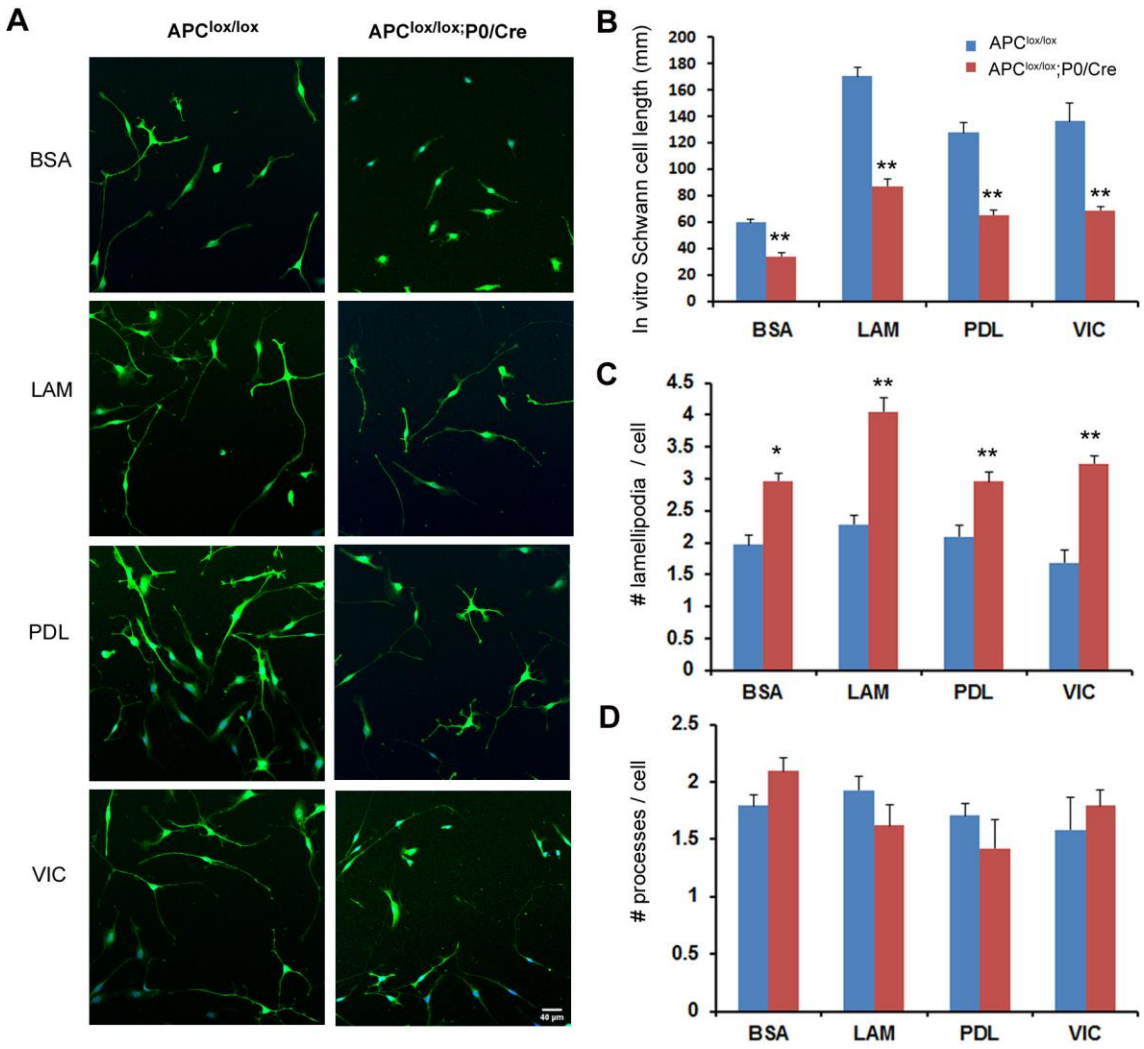


**Figure S6: The phenotype observed in the APC-ablated Schwann cells was β1 integrin-independent.** (A) Primary Schwann cells were cultured on either laminin, or the β1 integrin independent substrate vitronectin, or poly-D lysine, or BSA (used as control). The cells were fixed and stained for S100, a Schwann cell marker. The cell length (B), lamellipodia formation (C), and the number of processes (D), were all not affected by the plate coating material used, suggesting that the increased lamellipodia formation and perturbed processes extension observed in the APC-ablated Schwann cells was laminin/ β1 integrin-independent. The number of cells that were analyzed in vitro (primary culture): BSA: *Apc*$^{lox/lox}$: n=291, *Apc*$^{lox/lox}$;P0/Cre: n=353, laminin: *Apc*$^{lox/lox}$: n=272, *Apc*$^{lox/lox}$;P0/Cre: n=283, poly-D lysine: *Apc*$^{lox/lox}$: n=452, *Apc*$^{lox/lox}$;P0/Cre: n=373, vitronectin: *Apc*$^{lox/lox}$: n=367, *Apc*$^{lox/lox}$;P0/Cre: n=298 *p<0.05, **p<0.001.

**Movies**

**APC loss in Schwann cells results in hypomyelination and disrupted radial axonal sorting in the PNS.** *Apc$^{lox/lox}$;P0/Cre* mice exhibit reduced number of myelinated fibers, reduced myelin thickness and significantly shorter internodes (related to Fig. 2). *Apc$^{lox/lox}$;P0/Cre* mice also exhibit disrupted radial axonal sorting (related to Fig 3).

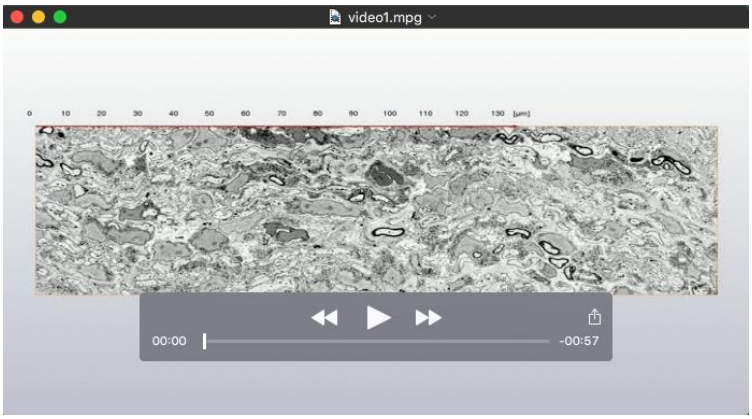


**Movie 1.** 3DEM images of serial longitudinal sections were acquired from sciatic nerves of P7 *Apc$^{lox/lox}$;P0/Cre* mice.

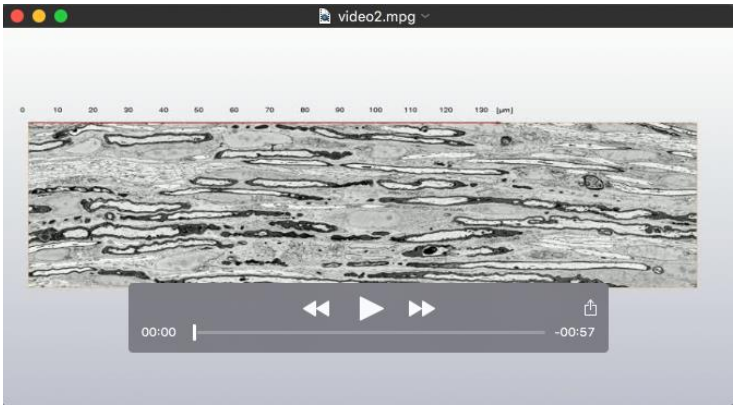


**Movie 2.** 3DEM images of serial longitudinal sections were acquired from sciatic nerves of P7 *Apc*$^{lox/lox}$ mice (control littermate) .

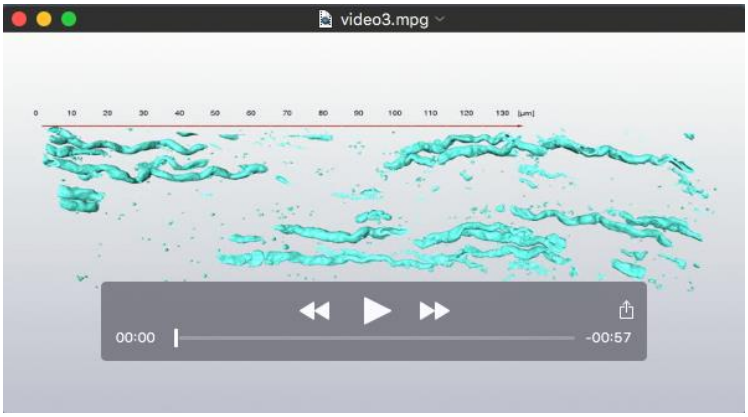


**Movie 3.** Myelin sheath shown in pseudocolor representation (cyan). Individual myelinated fibers were traced and analyzed on 3DEM images acquired from serial longitudinal sciatic nerve sections of P7 *Apc$^{lox/lox}$;P0/Cre* mice.

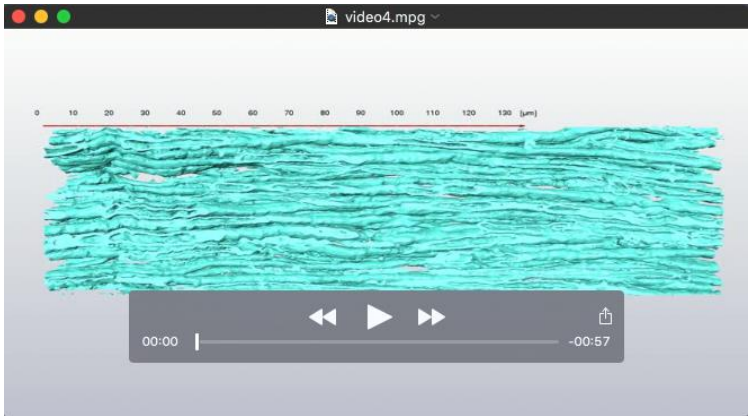


**Movie 4.** Myelin sheath shown in pseudocolor representation (cyan). Individual myelinated fibers were traced and analyzed on 3DEM images acquired from serial longitudinal sciatic nerve sections of P7 *Apc*$^{lox/lox}$ mice (control littermate).